Pergamon

Int. J. Solids Structures Vol. 34, No. 1, pp. 129–151, 1997

0020-7683/97 $15.00 + .00

0020-7683(95)00293-6

QUADRATIC TIME DOMAIN BEM FORMULATION FOR 2D ELASTODYNAMIC TRANSIENT ANALYSIS

CHUNG-CHENG WANG
Department of Civil Engineering, National Chiao Tung University, Hsinchu 30050, Taiwan

HUI-CHING WANG
Department of Applied Mathematics, National Chung Hsing University, Taichung 40203, Taiwan

and

GIN-SHOW LIOU
Department of Civil Engineering, National Chiao Tung University, Hsinchu 30050, Taiwan

(*Received* 11 *October* 1994; *in revised form* 22 *November* 1995)

Abstract—An accurate and efficient time domain BEM for the 2D elastodynamic wave transient analysis method is presented. Emphasis is focused on developing time domain fundamental convoluted kernels and methodology for quadratic temporal solution procedures which have never been presented before. In the presented BEM method, called the QC method, the temporal variations of displacement and traction are assumed to be quadratic and constant, respectively.

The spatial variations of displacement and traction fields are assumed to be quadratic. Also, the LC method, assuming linear temporal variation of displacement field and constant temporal variation of traction field, is examined in the paper. For the verification of the QC method, rectangular bars subject to different end loads are studied. The numerical results by the QC method are compared with analytical solutions and those by the LC method. Numerical study reveals that the QC method is more accurate and stable. In the QC method, a good numerical result can still be obtained even when $\beta = 1.0$–2.0. However $\beta = 0.50$–0.75 should be used in the LC method in order to obtain good numerical results. This would provide evidence that the QC method has great advantages over the LC method. Some conclusions regarding the QC method are also made.

1. INTRODUCTION

In recent years, the Boundary Element Method (BEM) has become increasingly popular for the solution of linear elastodynamic problems (Banerjee, 1994). Its popularity can be attributed primarily to the reduction of dimensionality of the problems, high accuracy of results and automatic consideration of the radiation conditions at infinity (Brebbia *et al.*, 1984).

In the early 1980s, Niwa *et al.* (1980) solved two-dimensional problems using three-dimensional transient kernels with the third spatial coordinate playing a role of time related variable. But Mansur (1983) was the first to formulate a time-stepping algorithm using 2D time-domain elasto-dynamic kernels. Later, Antes (1985) also employed a similar formulation. However, the accuracy of their formulation suffers from the following problems as indicated by Israil and Banerjee (1990b): mathematical complexity resulting from the treatment of Heaviside functions in the kernel functions, simplified assumptions of constant variation of spatial variables, modelling of boundary geometry by using straight line segments, and inadequate treatment of edges and corners, etc. These formulations are also called the first-generation direct time-domain BEM formulation for 2D transient dynamics (Israil and Banerjee, 1990b). Following this, integral equation solutions of elastodynamic problems in time domains have also been presented by the weighted residual method and the reciprocity method in 2D BEM formulations. Spyrakos and Antes (1986) have found that, for problems with short durations, the reciprocity method (same as Israil and Banerjee, 1990a) takes considerably less calculation time than that by the weighted residual method for elastodynamic transient problems. Recently, Israil and Banerjee

(1990a; 1990b; 1991) have made certain contributions to the numerical implementation of the time-stepping technique and also presented a number of numerical solutions. In all these works, the temporal convolution integrals are evaluated analytically and the spatial integrations are carried out numerically at each time step. Wang and Takemiya (1992) also obtained, analytically, both spatial and temporal integration for scalar wave by the Cagniard-De Hoop method.

Of all the aforementioned methods, temporal solution is assumed to be either the zeroth or first order (i.e., constant or linear variation) and one-time-step piecewise continuity. In this paper, the quadratic temporal solution (second order, two-time-step piecewise continuity) is developed for the first time. In this procedure, a quadratic temporal variation of displacement and a constant temporal variation of traction are assumed. The temporal integrations can be obtained analytically and the spatial integration is accomplished by using Gaussian quadrature. The technique of uniform subsegmentation is also used for the numerical integrations, since the kernels have singularities as well as jumps at the moving wave front.

As for wave fronts in which singularities exist in the sense of the Cauchy Principal Value, the finite part of the divergent integral are dodged in this paper by using rigid-body translation.

Several numerical examples are used to demonstrate the efficiency, effectiveness and numerical stability of the presented QC method. Some comparative studies are also made between the QC method and the LC method. In these studies, the dimensionless time step β is defined as

$$\beta \equiv \frac{c_1 \Delta t}{l} \tag{1}$$

where l is the element length, Δt is the time step used and c_1 is the pressure wave velocity. Banerjee (1994) has suggested that β should be between 0.5 and 0.75 in order to obtain an accurate solution. Since a larger β means less calculation cost if l in eqn (1) is fixed, the numerical investigation into β is also included in order to get an insight of numerical noise and accuracy of the results with respect to different β values. $0.5 \leqslant \beta \leqslant 4.0$ are used in the numerical examples.

2. BEM INTEGRAL REPRESENTATION FORMULAE

2.1. *Transient elastodynamics: governing equation*

The governing equation of dynamic equilibrium for an isotropic elastic homogeneous body is the so-called Navier's equation and can be written as

$$(\lambda+\mu)u_{j,ji}(\mathbf{x}, t) + \mu u_{i,jj}(\mathbf{x}, t) + \rho b_i(\mathbf{x}, t) = \rho \ddot{u}_i(\mathbf{x}, t) \tag{2}$$

where u_i is the component of displacement in the ith-direction, $\mathbf{x}$ is the position vector, t is the time variable, b_i is the component of the body force, λ and μ are the Lamé constants and ρ is the mass density of the material, and the inferior commas and overdot indicate space derivatives and time derivative, respectively.

Considering a domain V bounded by a surface S, the displacement at a point $\boldsymbol{\xi}$ and at time t can be obtained by the dynamic reciprocal work theorem in an integral form as

$$C_{ij}(\boldsymbol{\xi})u_j(\boldsymbol{\xi}, t) = \int_S \{G_{ij}(\boldsymbol{\xi}, \tau; \mathbf{x}, t) * t_j(\mathbf{x}, t) - F_{ij}(\boldsymbol{\xi}, \tau; \mathbf{x}, t) * u_j(\mathbf{x}, t)\}\, \mathrm{d}S(\mathbf{x})$$

$$+ \rho \int_V G_{ij}(\boldsymbol{\xi}, \tau; \mathbf{x}, t) * b_j(\mathbf{x}, t)\, \mathrm{d}V(\mathbf{x})$$

$$+\rho\int_V \{G_{ij}(\xi,\tau;\mathbf{x},t)\dot{u}_j(\mathbf{x},0)+\dot{G}_{ij}(\xi,\tau;\mathbf{x},t)u_j(\mathbf{x},0)\}\,\mathrm{d}V(\mathbf{x}). \quad (3)$$

In the above equation, ξ and $\mathbf{x}$ are source and receiver points, respectively, and $u_i(\mathbf{x},0)$ and $\dot{u}_i(\mathbf{x},0)$ are the initial displacement and velocity, respectively. $C_{ij}(\xi)$ is the well known discontinuity term which is dependent on local geometry. $*$ stands for the Reimann convolution integral (Eringen and Suhubi, 1975; Graff, 1975; Manolis and Beskos, 1988) and is defined by eqns (B1) and (B2) in Appendix B. The terms $G_{ij}(\xi,\tau;\mathbf{x},t)$ and $F_{ij}(\xi,\tau;\mathbf{x},t)$ are the fundamental solutions and represent, respectively, the displacement and traction at the field point $\mathbf{x}$ at time t due to a unit force applied at source point ξ at a preceding time τ. Equation (3) is valid for both bounded and unbounded regions which have been proved by De Hoop (1958) (Manolis and Beskos, 1988).

2.2. *Fundamental solution*

The desired 2D kernel in eqn (3) can be written for completeness as follows:

$$G_{ij}(\xi,\tau;\mathbf{x},t)=\frac{1}{2\pi\rho}\left\{\frac{H(c_1t'-r)}{c_1}\left[\frac{2\left(\frac{c_1t'}{r}\right)^2-1}{\sqrt{\left(\frac{c_1t'}{r}\right)^2-1}}\left(\frac{r_{,i}r_{,j}}{r}\right)-\frac{\delta_{ij}}{r}\sqrt{\left(\frac{c_1t'}{r}\right)^2-1}\right]\right.$$
$$\left.+\frac{H(c_2t'-r)}{c_2}\left[-\frac{2\left(\frac{c_2t'}{r}\right)^2-1}{\sqrt{\left(\frac{c_2t'}{r}\right)^2-1}}\left(\frac{r_{,i}r_{,j}}{r}\right)+\frac{\delta_{ij}}{r}\frac{\left(\frac{c_2t'}{r}\right)^2}{\sqrt{\left(\frac{c_2t'}{r}\right)^2-1}}\right]\right\} \quad (4)$$

where H is the Heaviside function, $t'=t-\tau$ is the retarded time, r denotes the distance $|\mathbf{x}-\xi|$, $c_1=\sqrt{(\lambda+2\mu)/\rho}$ and $c_2=\sqrt{\mu/\rho}$. The details of the derivation of eqn (4) can be found in the text by Eringen and Suhubi (1975), and similar forms can also be found in the works by Israil and Banerjee (1990a; 1991), Brebbia *et al.* (1984), Spyrakos and Beskos (1986), Antes (1985) and Dominguez and Gallego (1992). The F_{ij} kernel (the traction kernel) can also be obtained, using the strain–displacement relationship and the constitutive equations. The F_{ij} kernel is expressed as follows:

$$F_{ij}(\xi,\tau;\mathbf{x},t)=\frac{\mu}{2\pi\rho r}\left\{\frac{1}{c_1}H\left(\frac{c_1t'}{r}-1\right)\left[\frac{1}{\left\{\left(\frac{c_1t'}{r}\right)^2-1\right\}^{3/2}}\left(\frac{A_1}{r}\right)+\frac{2\left(\frac{c_1t'}{r}\right)^2-1}{\sqrt{\left(\frac{c_1t'}{r}\right)^2-1}}\left(\frac{2A_2}{r}\right)^{\dagger}\right]\right.$$
$$\left.-\frac{\delta(c_1t'-r)}{c_1}\left[(A_1)\frac{2\left(\frac{c_1t'}{r}\right)^2-1}{\sqrt{\left(\frac{c_1t'}{r}\right)^2-1}}-(B_2)\sqrt{\left(\frac{c_1t'}{r}\right)^2-1}\right]\right\}$$

† This term was erroneously typed by Israil and Banerjee (1990a; 1991; 1992) and Banerjee (1994) as

$$\frac{2\left(\frac{c_1t'}{r}\right)-1}{\sqrt{\left(\frac{c_1t'}{r}\right)^2-1}}\left(\frac{2A_2}{r}\right).$$

$$-\frac{1}{c_2}H\left(\frac{c_2t'}{r}-1\right)\left[\frac{1}{\left\{\left(\frac{c_2t'}{r}\right)^2-1\right\}^{3/2}}\left(\frac{A_3}{r}\right)+\frac{2\left(\frac{c_2t'}{r}\right)^2-1}{\sqrt{\left(\frac{c_2t'}{r}\right)^2-1}}\left(\frac{2A_2}{r}\right)\right]$$

$$+\frac{\delta(c_2t'-r)}{c_2}\left[(A_1)\frac{2\left(\frac{c_2t'}{r}\right)^2-1}{\sqrt{\left(\frac{c_2t'}{r}\right)^2-1}}-(B_2)\frac{\left(\frac{c_2t'}{r}\right)^2}{\sqrt{\left(\frac{c_2t'}{r}\right)^2-1}}\right]\Bigg\} \tag{5}$$

where

$$A_1=\left(\frac{\lambda}{\mu}\right)n_jr_{,i}+2r_{,i}r_{,j}\frac{\partial r}{\partial n} \tag{6}$$

$$A_2=n_ir_{,j}+n_jr_{,i}+\frac{\partial r}{\partial n}(\delta_{ij}-4r_{,i}r_{,j}) \tag{7}$$

$$A_3=\frac{\partial r}{\partial n}(2r_{,i}r_{,j}-\delta_{ij})-n_ir_{,j} \tag{8}$$

$$B_2=\frac{\lambda}{\mu}n_jr_{,i}+r_{,j}n_i+\delta_{ij}\frac{\partial r}{\partial n}. \tag{9}$$

The above expressions for the 2D transient F_{ij}-kernel are the most explicit and simplest among those that are available so far. Also, the terms involving the delta function $\delta(c_it'-r)$, representing the wave front contribution, are kept in the equation for completeness, although after spatial integration they make no contribution and were omitted by Israil and Banerjee (1990a).

3. NUMERICAL IMPLEMENTATION

For the numerical implementation of eqn (3), discretizations in both time and space domains are required. The time integrations can be performed analytically while the spatial integrations are treated numerically. The salient features of the temporal integrations and methodology will be presented.

In order to integrate the convolutions analytically, the time span of interest is discretized into N steps with duration Δt for one time step. Define $t_n=n\Delta t$ for $n=1, 2, \ldots, N$. The quadratic temporal variation of functions is developed by the same procedure as used in developing linear and constant temporal variations previously. All of the development of temporal interpolation functions is described in the following section.

3.1. *Temporal interpolation functions*

3.1.1. *Constant temporal interpolation functions.* If constant variation is assumed in one time step, then field variables can be expressed as:

$$f_i(\mathbf{x},\tau)=M_{CF}(\tau)f_i^n(\mathbf{x})+M_{CB}(\tau)f_i^{n-1}(\mathbf{x}) \tag{10}$$

where $f_i^n(\mathbf{x})$ stands for tractions (t_i^n) or displacements (u_i^n) at time step n and $M_{CF}(\tau)$ and $M_{CB}(\tau)$ are the constant temporal interpolation functions given by

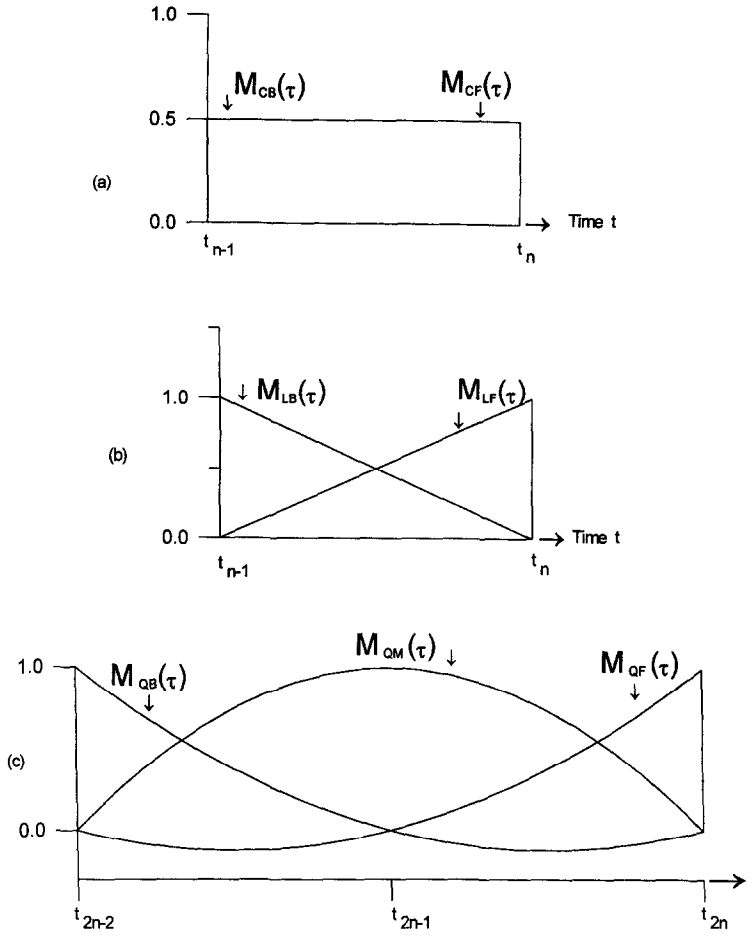

Fig. 1. Temporal various interpolation functions: (a) constant, (b) linear, (c) quadratic.

$$M_{CF}(\tau) = \tfrac{1}{2}, \quad M_{CB}(\tau) = \tfrac{1}{2}; \quad t_{n-1} \leqslant \tau \leqslant t_n, \tag{11}$$

in which the subscripts CF and CB are referred to the forward and backward temporal nodes, respectively, in a time step shown in Fig. 1(a).

3.1.2. *Linear temporal interpolation functions.* The field variables are approximated by using linear interpolation functions during one time step, and can be expressed as:

$$f_i(\mathbf{x}, \tau) = M_{LF}(\tau) f_i^n(\mathbf{x}) + M_{LB}(\tau) f_i^{n-1}(\mathbf{x}) \tag{12}$$

where $M_{LF}(\tau)$ and $M_{LB}(\tau)$ are linear temporal interpolation functions given by

$$M_{LF}(\tau) = \frac{\tau - t_{n-1}}{\Delta t}, \quad M_{LB}(\tau) = \frac{t_n - \tau}{\Delta t}; \quad t_{n-1} \leqslant \tau \leqslant t_n, \tag{13}$$

in which the subscripts LF and LB are referred to the forward and backward linear temporal nodes, respectively, in a time step shown in Fig. 1(b).

3.1.3. *Quadratic temporal interpolation functions.* The field variables are assumed to vary quadratically during two time steps, and can be expressed as:

$$f_i(\mathbf{x},\tau) = M_{QF}(\tau)f_i^{2n}(\mathbf{x}) + M_{QM}(\tau)f_i^{2n-1}(\mathbf{x}) + M_{QB}(\tau)f_i^{2n-2}(\mathbf{x}) \tag{14}$$

where $M_{QF}(\tau)$, $M_{QM}(\tau)$ and $M_{QB}(\tau)$ are quadratic temporal interpolation functions shown in Fig. 1(c) and can be given by:

$$M_{QF}(\tau) = \frac{1}{2}\left(\frac{\tau - t_{2n-2}}{\Delta t}\right)^2 - \frac{1}{2}\left(\frac{\tau - t_{2n-2}}{\Delta t}\right) \tag{15}$$

$$M_{QM}(\tau) = -\left(\frac{\tau - t_{2n-2}}{\Delta t}\right)^2 + 2\left(\frac{\tau - t_{2n-2}}{\Delta t}\right) \tag{16}$$

$$M_{QB}(\tau) = \frac{1}{2}\left(\frac{\tau - t_{2n-2}}{\Delta t}\right)^2 - \frac{3}{2}\left(\frac{\tau - t_{2n-2}}{\Delta t}\right) + 1 \quad \text{for } t_{2n-2} \leqslant \tau \leqslant t_{2n}, \tag{17}$$

in which the subscripts QF, QM and QB are referred to the forward, midpoint and backward temporal nodes, respectively, in two time steps ($2\Delta t$); i.e., a two-time-step piecewise continuous function.

3.2. *Temporal integration*

In evaluating the convoluted $G_{ij} * t_j$ and $F_{ij} * u_j$ kernels, the computational effort can be greatly reduced by making use of the time-translation property of the kernels. That is, at each time step, only the effect of the current time interval is needed to be evaluated. The traction convoluted kernels can be defined as follows:

$$[F_{CFij}^{N-n+1}] \equiv \int_{(n-1)\Delta t}^{n\Delta t} F_{ij}(\boldsymbol{\xi},\tau;\mathbf{x},N\Delta t)M_{CF}(\tau)\,\mathrm{d}\tau \tag{18}$$

$$[F_{CBij}^{N-n+1}] \equiv \int_{(n-1)\Delta t}^{n\Delta t} F_{ij}(\boldsymbol{\xi},\tau;\mathbf{x},N\Delta t)M_{CB}(\tau)\,\mathrm{d}\tau \tag{19}$$

$$[F_{LFij}^{N-n+1}] \equiv \int_{(n-1)\Delta t}^{n\Delta t} F_{ij}(\boldsymbol{\xi},\tau;\mathbf{x},N\Delta t)M_{LF}(\tau)\,\mathrm{d}\tau \tag{20}$$

$$[F_{LBij}^{N-n+1}] \equiv \int_{(n-1)\Delta t}^{n\Delta t} F_{ij}(\boldsymbol{\xi},\tau;\mathbf{x},N\Delta t)M_{LB}(\tau)\,\mathrm{d}\tau \tag{21}$$

$$[F_{QFij}^{2K-2n+2}] \equiv \int_{(2n-2)\Delta t}^{2n\Delta t} F_{ij}(\boldsymbol{\xi},\tau;\mathbf{x},2K\Delta t)M_{QF}(\tau)\,\mathrm{d}\tau \tag{22}$$

$$[F_{QMij}^{2K-2n+2}] \equiv \int_{(2n-2)\Delta t}^{2n\Delta t} F_{ij}(\boldsymbol{\xi},\tau;\mathbf{x},2K\Delta t)M_{QM}(\tau)\,\mathrm{d}\tau \tag{23}$$

$$[F_{QBij}^{2K-2n+2}] \equiv \int_{(2n-2)\Delta t}^{2n\Delta t} F_{ij}(\boldsymbol{\xi},\tau;\mathbf{x},2K\Delta t)M_{QB}(\tau)\,\mathrm{d}\tau. \tag{24}$$

Similarly, the displacement convoluted kernels can also be defined.

All these time convoluted kernel integrations can be carried out analytically. These procedures are similar to those of linear temporal variation described by Israil and Banerjee (1990a), except that the temporal functions in this paper are more complicated.

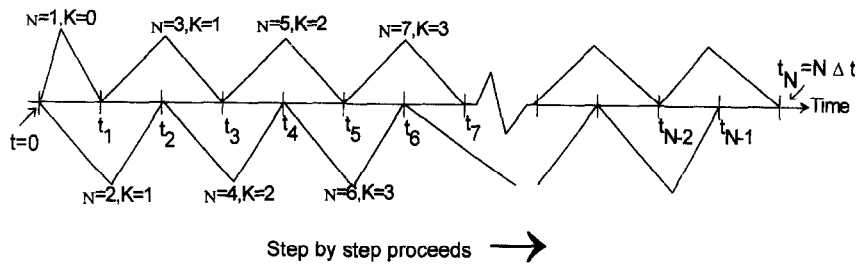

Fig. 2. Marching scheme used in the QC method.

3.3. *Step-by-step solution procedure*

It is of interest to note that eqn (3) is an implicit time-domain formulation, since the displacements at time t are being calculated by taking account of the history of surface tractions and the history of displacements up to time t. As mentioned before, the temporal variations of field variables (displacements and tractions) can be constant, linear and quadratic. The eqn (3) with zero initial conditions and absence of the body force for a certain temporal variation can be rewritten by using the discretization of time $t = N\Delta t$ as

$$C_{ij}(\xi)u_j^N(\xi) - \int_{(N-m)\Delta t}^{N\Delta t}\int_S ([G_{ij}t_j(\mathbf{x}) - F_{ij}u_j(\mathbf{x})])\,\mathrm{d}S(\mathbf{x})\,\mathrm{d}\tau = \int_0^{(N-m)\Delta t}\int_S ([G_{ij}t_j(\mathbf{x}) - F_{ij}u_j(\mathbf{x})])\,\mathrm{d}S(\mathbf{x})\,\mathrm{d}\tau = R^N, \quad (25)$$

in which $m = 1$ for constant and linear temporal variation, $m = 2$ for quadratic temporal variation and R^N represents the effect of past dynamic history on the current time node. After introducing the boundary conditions, eqn (25) becomes a system of $2M$ equations with $4M$ unknowns (M is the number of boundary nodes) for the first quadratic temporal step. Therefore, Brebbia *et al.* (1984) introduced an extra temporal node $t_{n-1/2}$ to double the total number of simultaneous equations involved in the first time step for 2D diffusion formulation. However, coupled simultaneous solution is needed and it appears to be difficult to solve. Therefore, only linear or constant variation is used in solving the field variables in first time step. In other words, first time step is the linear or constant step. After first time step, fully quadratic temporal solution procedure can then be established as shown in Fig. 2. Now, the solution procedure will be dependent upon whether N is even or odd.

(i) If N is even, let $N = 2K$. The following Reimann convolution can be obtained with more condensed manipulation in the following way:

$$\begin{aligned} F_{ij} * u_j &= \int_0^t F_{ij}(t-\tau)u_j(\mathbf{x},\tau)\,\mathrm{d}\tau = \int_0^{N\Delta t} F_{ij}(t-\tau)u_j(\mathbf{x},\tau)\,\mathrm{d}\tau \\ &= \sum_{n=1}^{K}\left\{\int_{2(n-1)\Delta t}^{2n\Delta t} F_{ij}(t-\tau)(M_{QF}u_j^{2n} + M_{QM}u_j^{2n-1} + M_{QB}u_j^{2n-2})\,\mathrm{d}\tau\right\} \\ &= \sum_{n=1}^{K}([F_{QFij}^{2K-2n+2} + F_{QBij}^{2K-2n}]u_j^{2n} + [F_{QMij}^{2K-2n+2}]u_j^{2n-1}). \end{aligned} \quad (26)$$

Using eqn (26) with the convoluted kernel functions described in eqns (18)–(24), eqn (25) becomes:

$$C_{ij}(\xi)u_j^{2K}(\xi) = \sum_{n=1}^{K}\int_S ([G_{QFij}^{2K-2n+2} + G_{QBij}^{2K-2n}]t_j^{2n}(\mathbf{x}) + [G_{QMij}^{2K-2n+2}]t_j^{2n-1}(\mathbf{x}) - [F_{QFij}^{2K-2n+2} + F_{QBij}^{2K-2n}]u_j^{2n}(\mathbf{x}) - [F_{QMij}^{2K-2n+2}]u_j^{2n-1}(\mathbf{x}))\,\mathrm{d}S(\mathbf{x}). \quad (27)$$

(ii) If N is odd, let $N = 2K+1$. Equation (25) similarly takes the form:

$$C_{ij}(\xi)u_j^{2K+1}(\xi) = \sum_{n=1}^{K}\int_S ([G_{QFij}^{2K-2n+2} + G_{QBij}^{2K-2n}]t_j^{2n+1}(\mathbf{x}) + [G_{QMij}^{2K-2n+2}]t_j^{2n}(\mathbf{x}) - [F_{QFij}^{2K-2n+2} + F_{QBij}^{2K-2n}]u_j^{2n+1}(\mathbf{x}) - [F_{QMij}^{2K-2n+2}]u_j^{2n}(\mathbf{x}))\,\mathrm{d}S(\mathbf{x}) + \int_S ([G_{LFij}^{2K+1} + G_{QBij}^{2K}]t_j^1(\mathbf{x}) - [F_{LFij}^{2K+1} + F_{QBij}^{2K}]u_j^1(\mathbf{x}))\,\mathrm{d}S(\mathbf{x}). \quad (28)$$

In the above two equations, $[G_{QFij}^{N-2n+2} + G_{QBij}^{N-2n}]$ and $[F_{QFij}^{N-2n+2} + F_{QBij}^{N-2n}]$ are the condensed quadratic convoluted kernels and are defined as follows:

$$[F_{QFij}^{2K-2n+2} + F_{QBij}^{2K-2n}] \equiv \int_{(2n-2)\Delta t}^{2n\Delta t} F_{ij}(\xi,\tau;\mathbf{x},2K\Delta t)M_{QF}(\tau)\,\mathrm{d}\tau + \int_{2n\Delta t}^{(2n+2)\Delta t} F_{ij}(\xi,\tau;\mathbf{x},2K\Delta t)M_{QB}(\tau)\,\mathrm{d}\tau. \quad (29)$$

In addition, the condensed quadratic convoluted displacement kernel and the condensed linear convoluted traction and displacement kernels can be similarly obtained.

It is worth noting that singularities exist in the various convoluted kernel functions $[F_{QFij}^2 + F_{QBij}^0]$, $[F_{LFij}^1 + F_{QBij}^0]$, $[F_{LFij}^1 + F_{LBij}^0]$, $[G_{CFij}^1 + F_{CBij}^0]$, $[G_{QFij}^2 + G_{QBij}^0]$ and $[G_{LFij}^1 + G_{QBij}^0]$, when the load point and the field point coincide ($\xi = \mathbf{x}$). The singularities in $[G_{QFij}^2 + G_{QBij}^0]$, $[G_{CFij}^1 + G_{CBij}^0]$ and $[G_{LFij}^1 + G_{QBij}^0]$ are in the form of $\ln r$ (weak singularity) and the singularities in others are in the form of $1/r$ (strong singularity). One should also note that only the first piecewise continuous function is a one time step function and the other piecewise functions are two-time-step functions. The last integral form in eqn (28) represents the first time step effect which includes parts of linear variation contribution and parts of quadratic variation contribution. Moreover, the fully condensed quadratic convoluted kernels of eqn (28) apparently equal that of eqn (27).

It should be recognized that the temporal variations of displacements and tractions can be different. Two mixed methods (i.e., different temporal variations for displacement and traction) are introduced as follows.

3.3.1. *QC method solution procedure.* The mixed solution procedure is developed to combine different temporal displacement variations and traction variations. It is easier to mix a constant variation of traction with a quadratic variation of displacement. In most of the available analytical solutions of transient problems, the temporal variations of tractions are constant. So, two different methods are introduced as follows. One uses constant temporal variation of traction and quadratic temporal variation of displacement. This is called the QC method in the paper. The other uses constant temporal variation of traction and linear temporal variation of displacement. This is called the LC method in the paper. Only the constant temporal variation of traction in one time step is currently developed. The mixed variation procedure can similarly be obtained as quadratic variation procedure described in the last section through simple manipulations. However, it is important to discern constant variation of a linear step from constant variation of a quadratic step.

Hence, the constant convoluted displacement kernels with quadratic temporal step is expressed in terms equivalent to constant convoluted displacement kernels with linear temporal step which are shown in eqns (A1), (A2) and (A3) of Appendix A. And the

condensed quadratic convoluted traction kernels with quadratic temporal step are shown in eqns (A4), (A5) and (A6) of Appendix A. In the above mentioned convoluted kernels, the time-related terms are always non-negative because of the causality property of the wave. Also, because of the time-translation property, the convoluted kernels need to be evaluated only for $n = 1$ (Banerjee, 1994).

The QC method solution procedure can be similarly obtained by using eqns (27), (28) and replacing linear variation of $[G^{2K+1}_{LFij} + G^{2K}_{QBij}]$ with constant variation of $[G^{2K+1}_{CFij} + G^{2K}_{CBij}]$ as follows:

(i) If N is even, let $N = 2K$.

$$C_{ij}(\xi)u_j^{2K}(\xi) = \sum_{n=1}^{K} \int_S ([G^{2K-2n+1}_{CFij} + G^{2K-2n}_{CBij}]t_j^{2n}(\mathbf{x}) + [G^{2K-2n+2}_{CFij} + G^{2K-2n+1}_{CBij}]t_j^{2n-1}(\mathbf{x}) - [F^{2K-2n+2}_{QFij} + F^{2K-2n}_{QBij}]u_j^{2n}(\mathbf{x}) - [F^{2K-2n+2}_{QMij}]u_j^{2n-1}(\mathbf{x}))\, \mathrm{d}S(\mathbf{x}). \quad (30)$$

(ii) If N is odd, let $N = 2K+1$.

$$C_{ij}(\xi)u_j^{2K+1}(\xi) = \sum_{n=1}^{K} \int_S ([G^{2K-2n+1}_{CFij} + G^{2K-2n}_{CBij}]t_j^{2n+1}(\mathbf{x}) + [G^{2K-2n+2}_{CFij} + G^{2K-2n+1}_{CBij}]t_j^{2n}(\mathbf{x}) - [F^{2K-2n+2}_{QFij} + F^{2K-2n}_{QBij}]u_j^{2n+1}(\mathbf{x}) - [F^{2K-2n+2}_{QMij}]u_j^{2n}(\mathbf{x}))\, \mathrm{d}S(\mathbf{x}) + \int_S ([G^{2K+1}_{CFij} + G^{2K}_{CBij}]t_j^{1}(\mathbf{x}) - [F^{2K+1}_{LFij} + F^{2K}_{QBij}]u_j^{1}(\mathbf{x}))\, \mathrm{d}S(\mathbf{x}). \quad (31)$$

3.3.2. *LC mixed method solution procedure.* For the LC method, the solution procedure can be expressed as follows:

$$C_{ij}(\xi)u_j^{N}(\xi) = \sum_{n=1}^{N} \int_S ([G^{N-n+1}_{CFij} + G^{N-n}_{CBij}]t_j^{n}(\mathbf{x}) - [F^{N-n+1}_{LFij} + F^{N-n}_{LBij}]u_j^{n}(\mathbf{x}))\, \mathrm{d}S(\mathbf{x}) \quad (32)$$

where subscripts LF and LB are the forward and backward temporal nodes of linear time step as depicted in Fig. 1b, respectively.

3.4. *Spatial divergent integral*

However, the convoluted $F_{ij} * u_j$ kernels contain the strong singular terms that cause difficulty in numerical integration especially for a mesh with widely varying element lengths (Israil and Banerjee, 1990b). But, after convoluted kernels are condensed as demonstrated in eqn (28), those strong singularity terms cancel each other and result in well-behaved functions for $N > 2$. And only for $N = 1$ (for linear temporal variation) and $N = 2$ (for quadratic temporal variation) strong singularity of $O(1/r)$ exists at wave fronts. Furthermore, the condensed kernels form in eqns (27) and (28) can save computer memory space by merging two arrays into one array.

The divergent integral in the sense of Cauchy Principal Value (Chen and Zhou, 1992) is evaluated in the following way (Israil and Banerjee, 1990b):

$$\int_S F_{ij}^{trans}\, \mathrm{d}S = \int_S F_{ij}^{static}\, \mathrm{d}S + \int_S (F_{ij}^{trans} - F_{ij}^{static})\, \mathrm{d}S. \quad (33)$$

The first integral on the right hand side of eqn (33) is divergent and its evaluation using the technique of rigid body motions is well known. The second integral of eqn (33) is non-singular and can be evaluated numerically without difficulty.

4. BEHAVIOR OF TRANSIENT CONVOLUTED KERNELS AT A LARGE TIME STEP

The property of reducing the convoluted kernels of elastodynamics to the corresponding elastostatic kernels, when the time step is large, is very important for checking the convoluted kernels. The mathematical proof of this property for quadratic and constant temporal variation are given as follows.

From the following relationship

$$\left(\frac{1}{c_1^2}+\frac{1}{c_2^2}\right)=\frac{3-4\nu}{2(1-\nu)c_2^2} \quad \text{and} \quad \left(\frac{1}{c_2^2}-\frac{1}{c_1^2}\right)=\frac{1}{2(1-\nu)c_2^2}, \tag{34}$$

one can easily derive the following useful formula

$$\text{as} \quad \left(\frac{c_i\Delta t}{r}\right)\gg 1, \quad \left\{\frac{\cosh^{-1}\left(\frac{c_1\Delta t}{r}\right)}{c_1^2}+\frac{\cosh^{-1}\left(\frac{c_2\Delta t}{r}\right)}{c_2^2}\right\}\approx\frac{\ln\left(\frac{2c_1\Delta t}{r}\right)}{c_1^2}+\frac{\ln\left(\frac{2c_2\Delta t}{r}\right)}{c_2^2}$$

$$=\frac{\ln\left(\frac{1}{r}\right)}{c_1^2}+\frac{\ln\left(\frac{1}{r}\right)}{c_2^2}+\frac{\overbrace{\ln(2c_1\Delta t)}^{\text{constant}}}{c_1^2}+\frac{\ln(2c_2\Delta t)}{c_2^2}=\frac{3-4\nu}{2(1-\nu)c_2^2}\ln\left(\frac{1}{r}\right)+\text{constant} \tag{35}$$

$$\text{If } |x|\ll|a|, \quad \text{then} \quad (a^2-x^2)^{1/2}\approx\left(a-\frac{1}{2a}(x)^2\right). \tag{36}$$

These formulae will be used for proving the property mentioned above for each convoluted kernel in the following subsections. The transient condensed quadratic convoluted kernels as shown in eqn (A5) at a large time step are studied first. For $K=1$, the kernel $[F^2_{QFij}+F^0_{QBij}]$ can be written as

$$\begin{aligned}[F^2_{QFij}+F^0_{QBij}]=\frac{\mu}{2\pi\rho r}\Bigg\{&\left(\frac{2A_1+A_2}{4c_1^2}\right)\left(\frac{r}{c_1\Delta t}\right)^2\left[\cosh^{-1}\left(\frac{2c_1\Delta t}{r}\right)\right]\\&-\left(\frac{A_1}{2c_1^2}\right)\left[\sqrt{(2)^2-\left(\frac{r}{c_1\Delta t}\right)^2}\right]+\left(\frac{A_2}{6c_1^2}\right)\left[-(3)\sqrt{(2)^2-\left(\frac{r}{c_1\Delta t}\right)^2}\right]\\&-\left(\frac{2A_3+A_2}{4c_2^2}\right)\left(\frac{r}{c_2\Delta t}\right)^2\left[\cosh^{-1}\left(\frac{2c_2\Delta t}{r}\right)\right]+\left(\frac{A_3}{2c_2^2}\right)\left[\sqrt{(2)^2-\left(\frac{r}{c_2\Delta t}\right)^2}\right]\\&-\left(\frac{A_2}{6c_2^2}\right)\left[-(3)\sqrt{(2)^2-\left(\frac{r}{c_2\Delta t}\right)^2}\right]\Bigg\}.\end{aligned} \tag{37}$$

Substituting eqns (35)–(36) into eqn (37) and assuming $c_i\Delta t/r\to\infty$, the following can be obtained:

$$\lim_{c_i\Delta t/r\to\infty}[F^2_{QFij}+F^0_{QBij}]$$

$$=\frac{\mu}{2\pi\rho r}\left\{-\left(\frac{A_1}{2c_1^2}\right)[(2)]+\left(\frac{A_2}{6c_1^2}\right)[-(3)(2)]+\left(\frac{A_3}{2c_2^2}\right)[(2)]-\left(\frac{A_2}{6c_2^2}\right)[-(3)(2)]\right\}$$

$$=\frac{\mu}{2\pi\rho r}\left\{-\left(\frac{A_1}{c_1^2}\right)+\left(\frac{A_3}{c_2^2}\right)+A_2\left(\frac{1}{c_2^2}-\frac{1}{c_1^2}\right)\right\}$$

$$= \frac{-1}{4\pi(1-\nu)r}\left\{\frac{\partial r}{\partial n}((1-2\nu)\,\delta_{ij}+2r_{,i}r_{,j})-(1-2\nu)(r_{,i}n_j-r_{,j}n_i)\right\}$$

$$= \text{Kelvin's 2D traction fundamental solution of elastostatics.} \tag{38}$$

The same behavior can be proven for $[F^1_{LFij}+F^0_{QBij}]$ and $[F^1_{LFij}+F^0_{LBij}]$.

Similarly, the behavior of the middle point convoluted kernel $[F^2_{QMij}]$ can be reduced from eqn (A6).

$$[F^2_{QMij}] = \frac{\mu}{2\pi\rho r}\left\{+\left(\frac{2A_2}{3}\right)\left(\frac{\Delta t}{r}\right)^2\left[+4\sqrt{(2)^2-\left(\frac{r}{c_1\Delta t}\right)^2}\right]\right.$$
$$+\left(\frac{A_2}{3c_1^2}\right)\left[+1\sqrt{(2)^2-\left(\frac{r}{c_1\Delta t}\right)^2}\right]+\left(\frac{2A_1+A_2}{2c_1^2}\right)\left(\frac{r}{c_1\Delta t}\right)^2\left[-\cosh^{-1}\left(\frac{2c_1\Delta t}{r}\right)\right]$$
$$-\left(\frac{2A_2}{3}\right)\left(\frac{\Delta t}{r}\right)^2\left[+4\sqrt{(2)^2-\left(\frac{r}{c_2\Delta t}\right)^2}\right]-\left(\frac{A_2}{3c_2^2}\right)\left[+\sqrt{(2)^2-\left(\frac{r}{c_2\Delta t}\right)^2}\right]$$
$$\left.-\left(\frac{2A_3+A_2}{2c_2^2}\right)\left(\frac{r}{c_2\Delta t}\right)^2\left[-\cosh^{-1}\left(\frac{2c_2\Delta t}{r}\right)\right]\right\}. \tag{39}$$

Therefore, the following result can be concluded as $c_i\Delta t/r\to\infty$.

$$\lim_{c_i\Delta t/r\to\infty}[F^2_{QMij}] = \frac{\mu}{2\pi\rho r}\left\{+\left(\frac{2A_2}{3c_1^2}\right)\left[-\frac{4}{(2)(2)}\right]+\left(\frac{A_2}{3c_1^2}\right)[2]\right.$$
$$\left.-\left(\frac{2A_2}{3c_2^2}\right)\left[-\frac{4}{(2)(2)}\right]-\left(\frac{A_2}{3c_2^2}\right)[2]\right\}=0. \tag{40}$$

For $K>1$, one can find in eqn (A5) of Appendix A that all of sums of these terms having same coefficient are zeroes as $c_i\Delta t/r\to\infty$, i.e.,

$$-\left(\frac{A_1}{2c_1^2}\right)[(2K-1)(2K)-6(2K-2)-(2K-3)(2K-4)]=0, \tag{41}$$

$$+\left(\frac{A_3}{2c_2^2}\right)[(2K-1)(2K)-6(2K-2)-(2K-3)(2K-4)]=0 \tag{42}$$

and

$$+\left(\frac{A_2}{6c_i^2}\right)[-(5K-2)(2K)+12(2K-2)+(5K-8)(2K-4)]$$
$$-\left(\frac{A_2}{3c_i^2}\right)\left[(K-1)(2K)^2\left(\frac{(1)}{(2K)(2)}\right)-6(2K-2)^2\left(\frac{(1)}{(2K-2)(2)}\right)\right.$$
$$\left.-(K-1)(2K-4)^2\left(\frac{(1)}{(2K-4)(2)}\right)\right]=0. \tag{43}$$

This means that $\lim_{(c_i\Delta t/r)\to\infty}[F^{2K}_{QFij}+F^{2K-2}_{QBij}]=0$ for $K>1$. Only $K=1$ and, similarly, for $N=1$, have strong singularities. However, as $c_i\Delta t/r\to\infty$, the convoluted kernels are exactly reduced to the corresponding elastostatic kernels. Similarly, through a limiting process, the

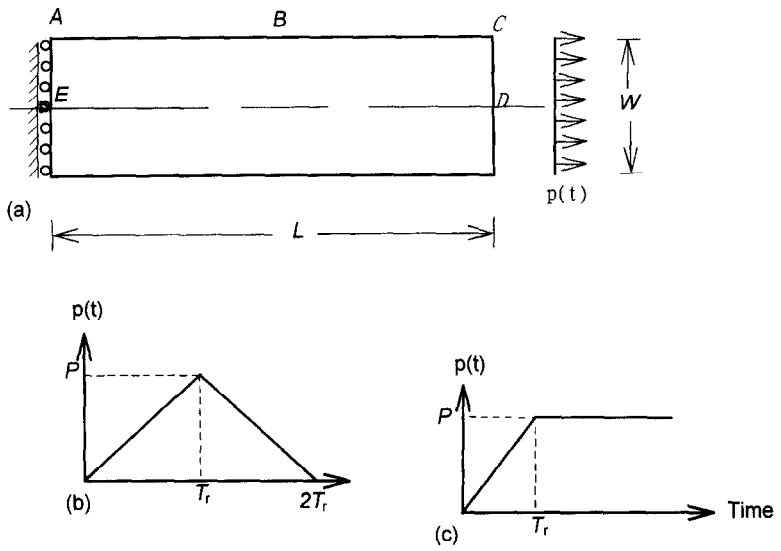

Fig. 3. Rectangular bar subjected to prescribed loading: (a) geometry and BCs, (b) triangular loading, (c) ramp-step loading.

same conclusion of reduction to elastostatic kernels can be brought for the case of convoluted displacement kernels.

5. NUMERICAL ANALYSIS

The following examples are presented in order to demonstrate the capability of the developed time-convoluted BEM algorithm. The geometry is modelled with continuous isoparametric quadratic elements. In the model, the components of surface traction (or reaction) can be different on both elements attached to the same corner node. First, to show the convergence of the QC method, a rectangular bar subject to a triangular load is considered by using different meshes and different time step sizes. Then a different rectangular bar subject to ramp-step load is analyzed again for verification.

For comparisons of numerical results, the same integration scheme is used for both the QC method and the LC method. Since the spatial variations of the convoluted kernels are very complex functions which are logarithmic functions and square root functions, a uniform subsegmentation technique is adopted in the evaluation of these spatial integrals. Each boundary element is divided into 12 and 8 subsegments in the integration of singular and regular kernels, respectively. Besides, 32 Gaussian points on each subsegment are used for a singular integration and 10 Gaussian points on each subsegment for a regular integration.

5.1. *Bar subjected to triangular load*

A rectangular bar (see Fig. 3a), whose length L is twice its width W, is fixed at its left end with traction free on its top and bottom sides. The Poisson's ratio is assumed to be zero. The right end side of bar is uniformly subjected to a triangular and tensile load (see Fig. 3) which increases from zero at time $t = 0$ to P at $t = T_r = L/c_1$ and then decreases to zero at $t = 2T_r$. Thus, the solution is pure 1D solution and the primary wave front just reaches the fixed end at time $t = T_r$ and bounces back to the right end at $t = 2T_r$. The material constants are $E = 7.8$, $\nu = 0$ and $c_1 = 100$.

To show the convergence of the QC method, three different discretized meshes (see Fig. 4) are chosen for the same time-step size $\beta = 0.5$. Among the three meshes, one is course mesh with 12 nodes and 6 quadratic elements, another is moderate mesh with 32 nodes and 16 quadratic elements, and the other is fine mesh with 48 nodes and 24 quadratic elements. The axial displacement (u) at point C and the horizontal reaction (R) at point A (see Fig. 3a) is investigated. The numerical results by the QC method are compared with

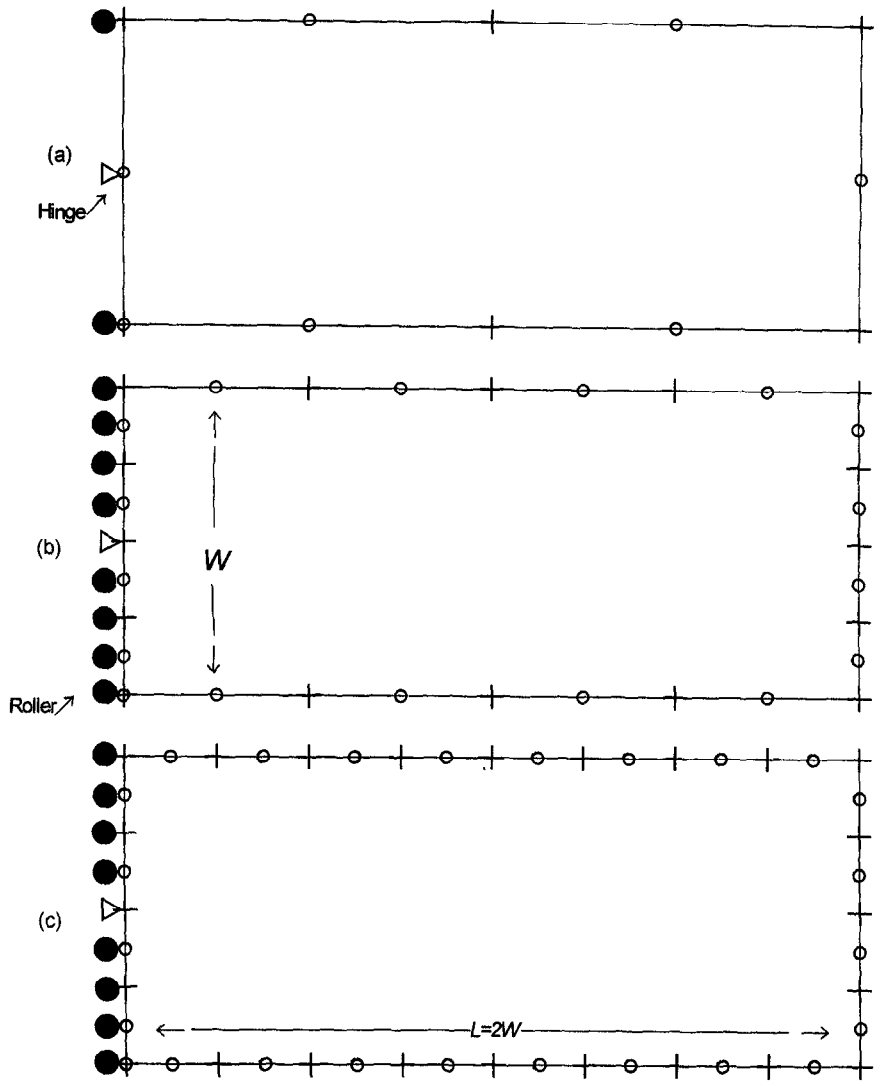

Fig. 4. Various discretization of the bar ($L/W = 2$): (a) 12 nodes and 6 quadratic elements, (b) 32 nodes and 16 quadratic elements, (c) 48 nodes and 24 quadratic elements.

that of analytical solution for $\beta = 0.5$ in Figs 5 and 6. From these figures, one can see that all three types of mesh give very good results and that the finer mesh gives the better results.

Furthermore, in order to understand how time-step size affects the accuracy of the QC method, four different time-step sizes ($\beta = 0.5$, 1, 2 and 4) are chosen in the solution procedure. The results with the four time-step sizes by the QC method using the mesh of 32 nodes are also plotted together in Figs 5 and 6. Apparently, the smaller β is used, the better results are obtained.

For comparison of accuracy between the QC method and the LC method, the mesh of 32 nodes is again used for analysis. From Figs 7 and 8, at the beginning ($c_1 t/L < 4$), both the QC method and the LC method agree very well with analytical solution. As time increases, the difference between the numerical solution and analytical solution starts to be observed and as time increases further, the differences become bigger. However, the QC method is much more accurate than the LC method. Especially, the peak value of the traction by the LC method reduce very fast as time increases.

Note that this reduction of peak values of displacements and tractions also occurs in the QC method. This erroneous damping effect is generally regarded as numerical damping. It may be caused by use of a large time step which can reduce the elastodynamic kernels into the elastostatic kernels proven in Section 4. This error can be reduced by using a

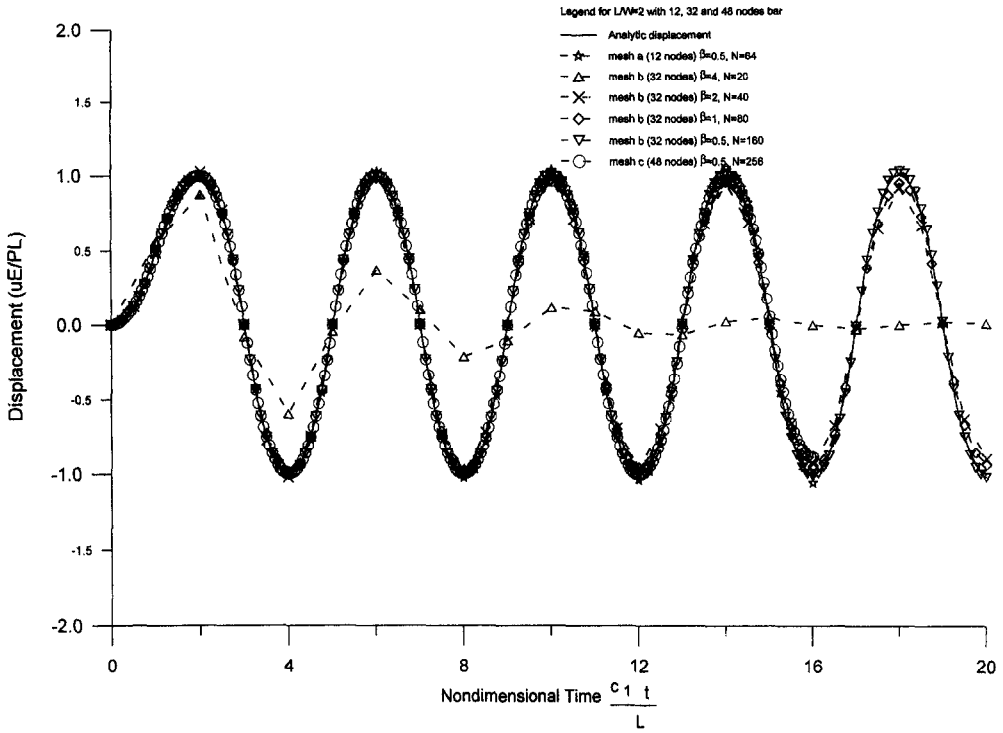

Fig. 5. Comparison QC method of displacement at point C for $\beta = 0.5$–4.0 under triangular loading.

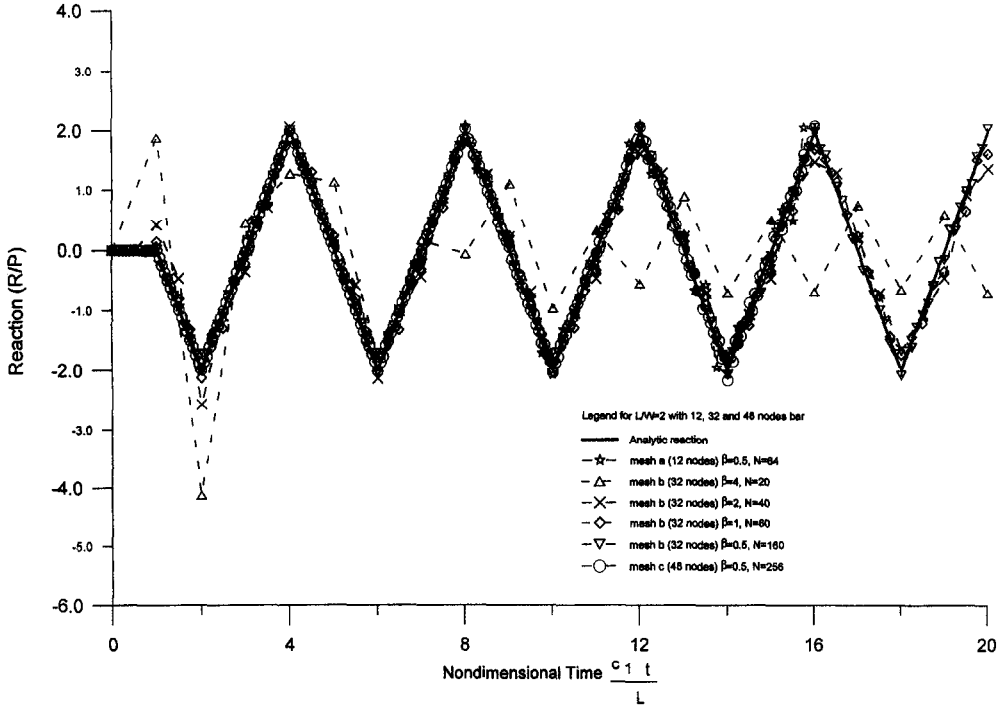

Fig. 6. Comparison QC method of reaction at point A for $\beta = 0.5$–4.0 under triangular loading.

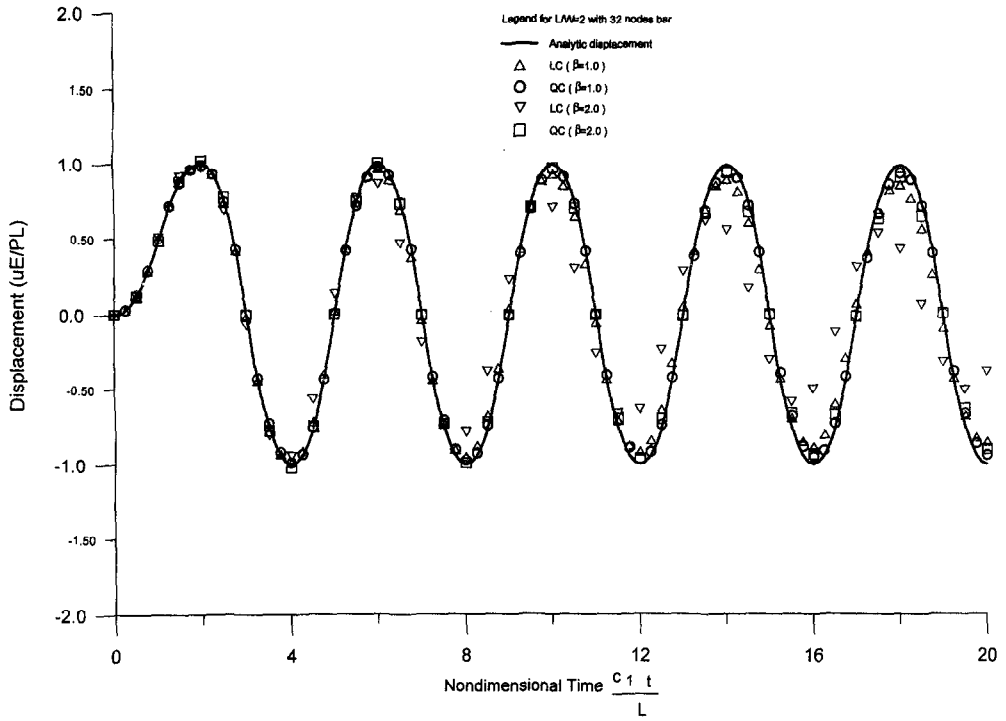

Fig. 7. Comparison of displacement at point C for $\beta = 1.0$ and 2.0 under triangular loading.

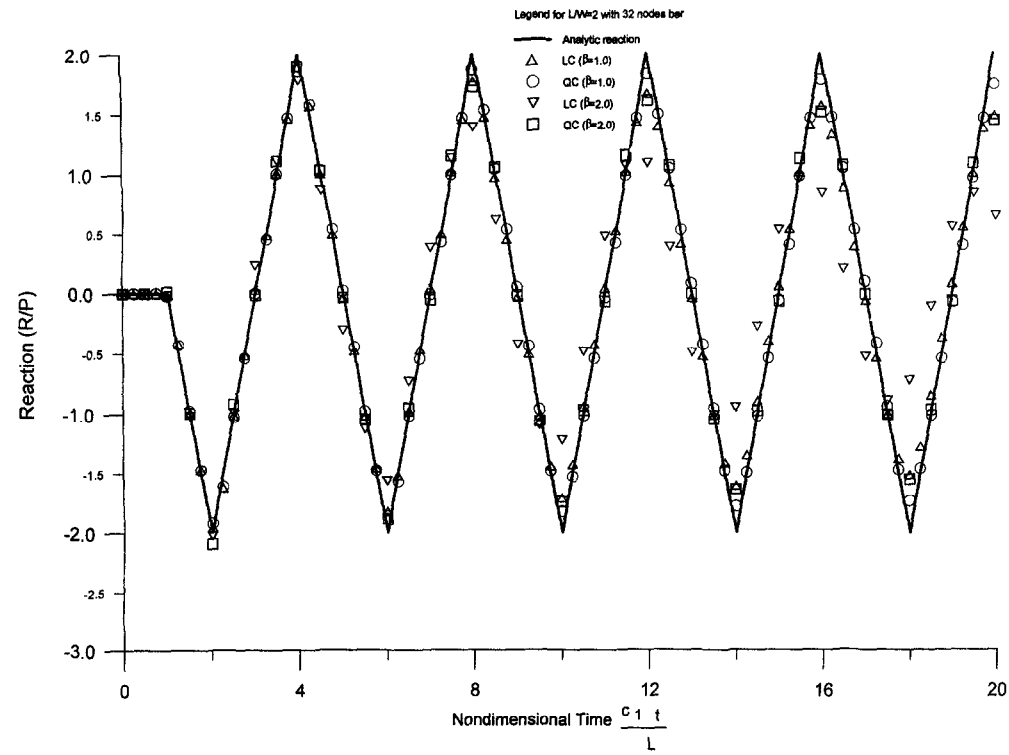

Fig. 8. Comparison of the QC with the LC method at point A for $\beta = 1.0$ and 2.0 under a triangular loading.

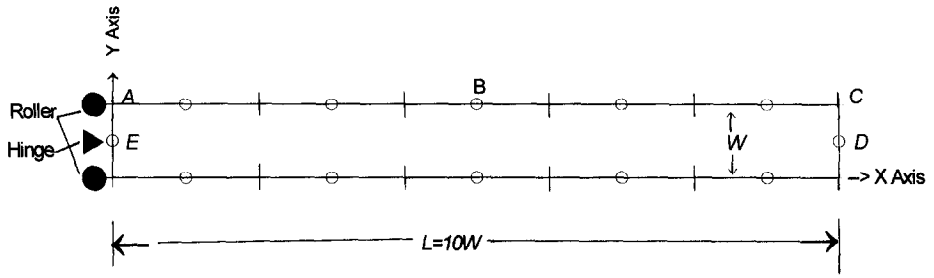

Fig. 9. Boundary element discretization of a rectangular bar, $L/W = 10$, 24 nodes, 12 quadratic elements.

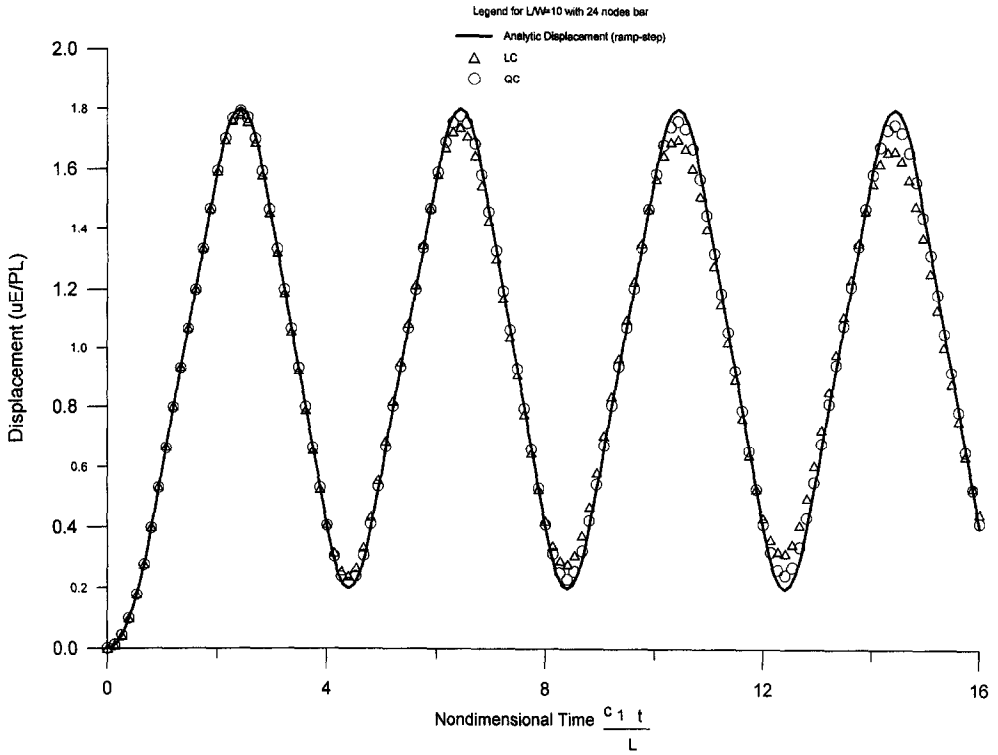

Fig. 10. Comparison of displacement at point C for $\beta = 2/3$ under ramp-step loading.

smaller time step size. However, a smaller time step size means more time steps and more accumulation of numerical errors. So, too small time step size sometimes should be avoided.

5.2. *A bar subjected to uniform ramp-step load*

The same rectangular bar, except length-to-width ratio $L/W = 10$, subjected to a ramp-step load as shown in Fig. 3 is used in the investigation of the presented method (QC method). The boundary conditions and its material constants are the same as those in the previous example. The boundary is discretized into twelve quadratic boundary elements as shown in Fig. 9.

Under the ramp-step load, the magnitude of the applied load starts linearly increasing from zero and then is kept constant after time $t = T_r = 0.8L/c_1$.

Again, four different time-step sizes (2/3, 1.0, 4/3 and 2) are used in the analyses. It means that when $t = T_r$, the wave front just arrives at the point $0.2L$ away from the fixed end.

The displacement at point C and the reaction at point A is still investigated. The numerical solutions by the QC method and the LC method are plotted together and compared to the analytical solution in Figs 10–16. Again, the numerical damping is observed in the figures. From these figures, the QC method is still much better and more accurate

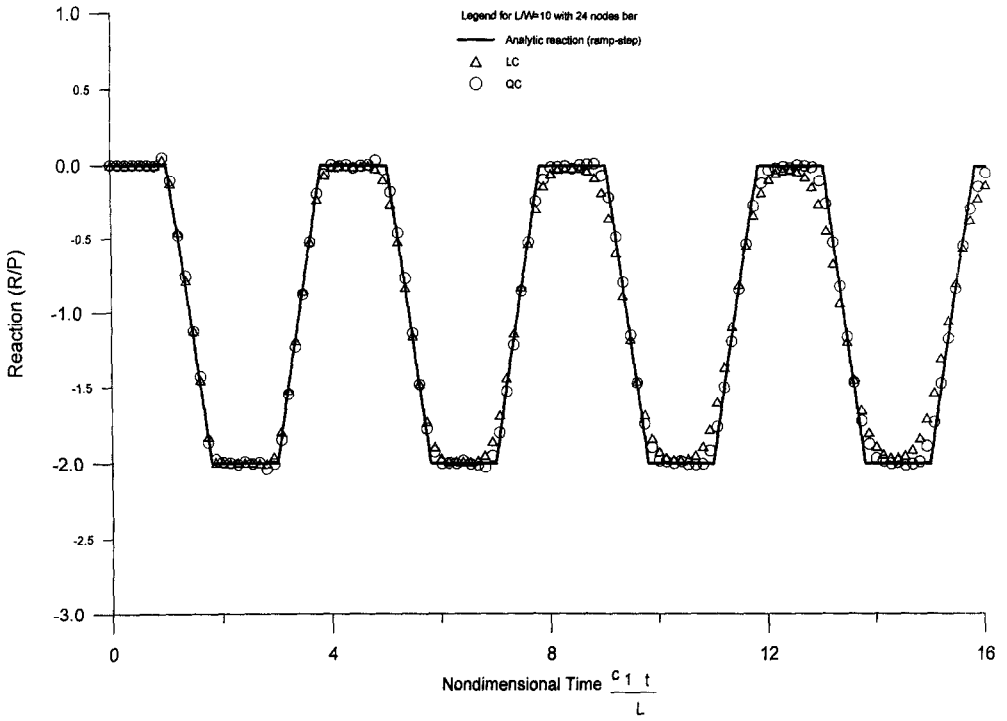

Fig. 11. Comparison of reaction at point A for $\beta = 2/3$ under ramp-step loading.

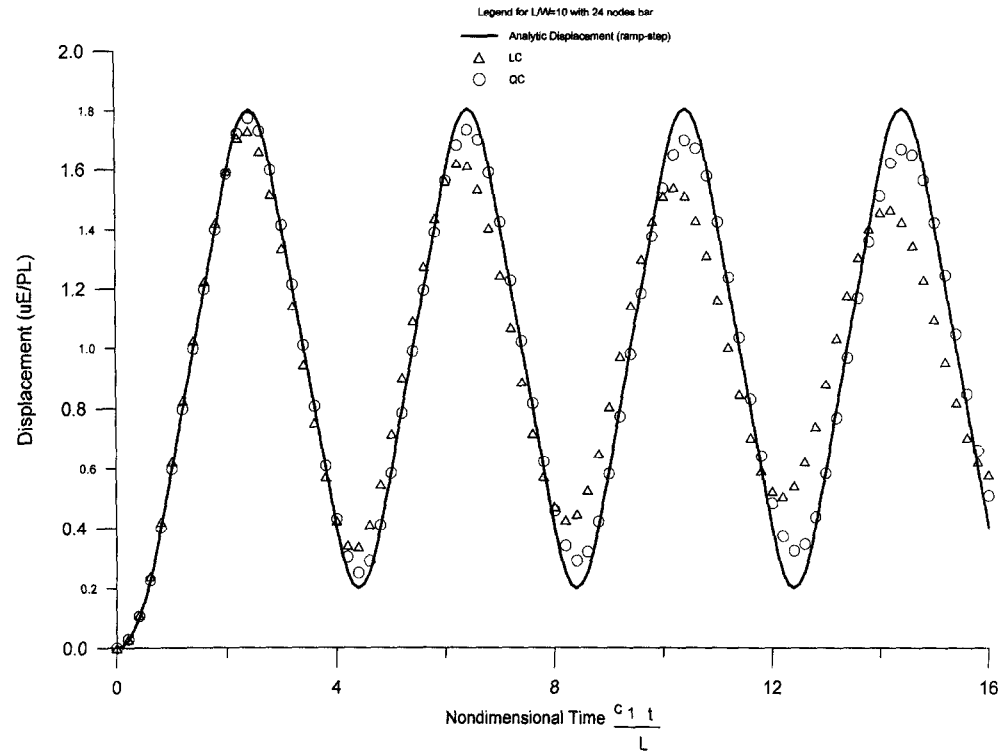

Fig. 12. Comparison of displacement at point C for $\beta = 1.0$ under ramp-step loading.

than the LC method depicted in Figs 10–16. Particularly, when $\beta = 4/3$ or 2, both the displacement and traction at corner points (point A and C) by the LC method go divergent (see Figs 14–16). Basically, it agrees with the fact concluded by Banerjee (1994) that the value of β should be 0.5–0.75 for best results and shouldn't be greater than 1.0.

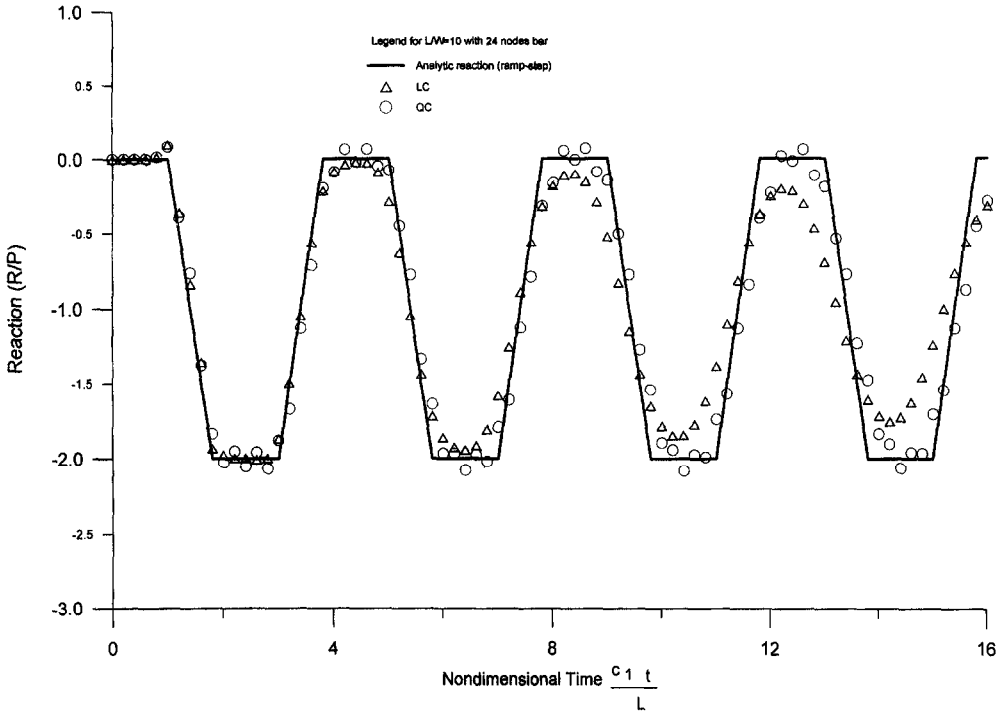

Fig. 13. Comparison of reaction at point A for $\beta = 1.0$ under ramp-step loading.

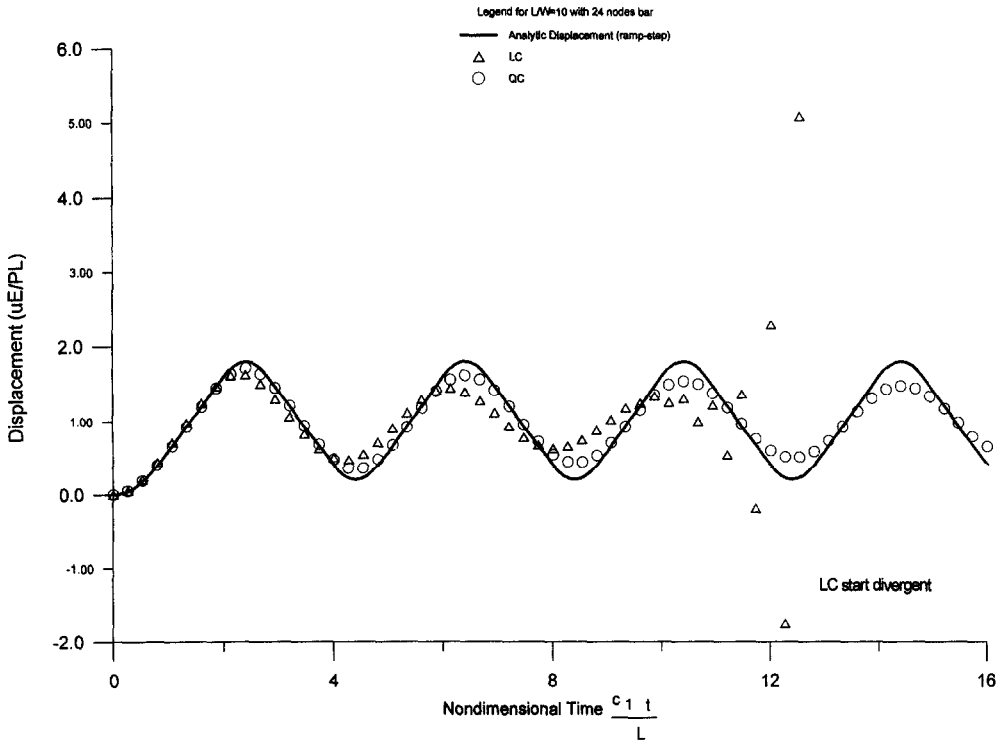

Fig. 14. Comparison of displacement at point C for $\beta = 4/3$ under ramp-step loading.

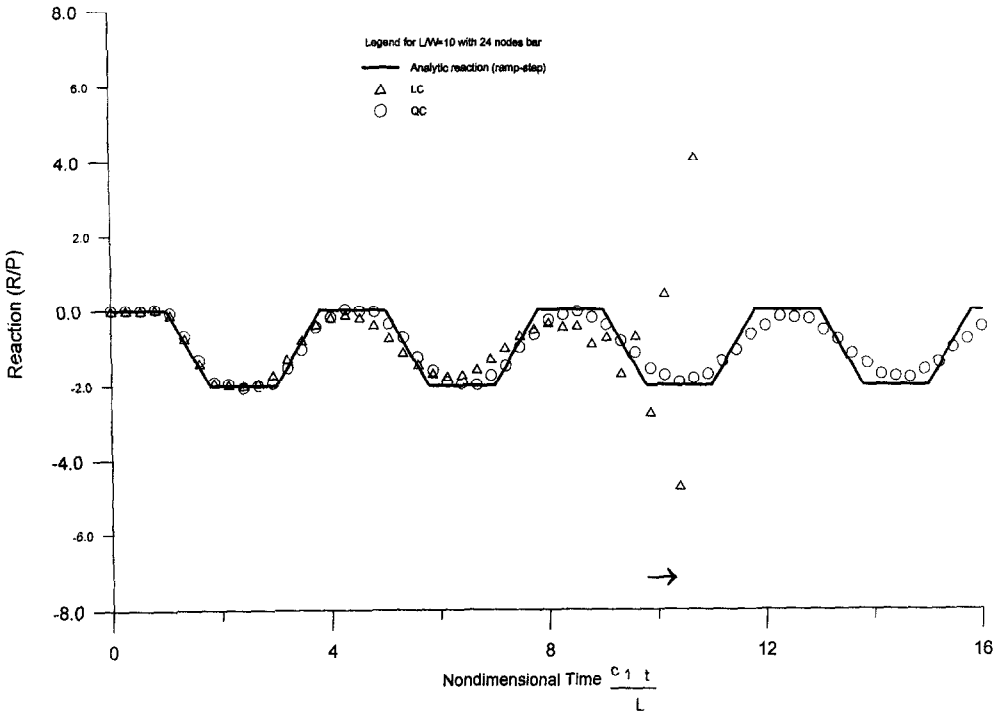

Fig. 15. Comparison of reaction at point A for $\beta = 4/3$ under ramp-step loading.

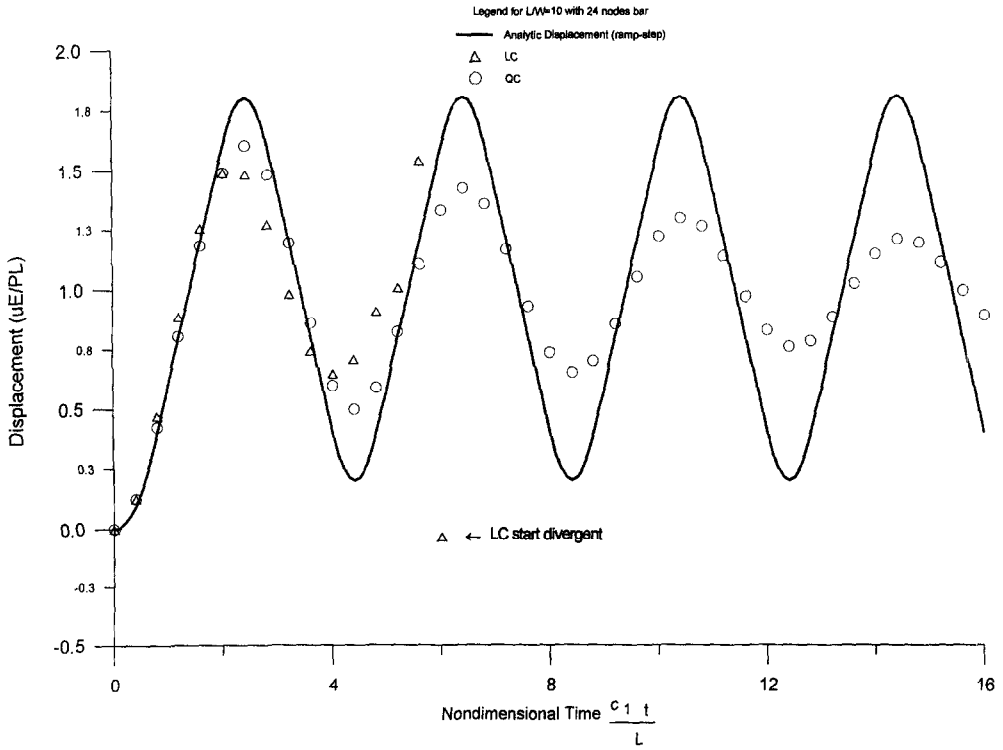

Fig. 16. Comparison of displacement at point C for $\beta = 2.0$ under ramp-step loading.

6. CONCLUSION

After some extensive numerical studies of the presented BEM scheme, the following conclusions can be drawn.

(1) The presented QC method can be easily programmed. A computer program for elastostatics can be easily modified to the computer program for elastodynamic problems by simply changing kernel functions and sequential solution procedure of eqns (30) and (31).

(2) The QC method has been compared with the LC method in several example problems under the same integration scheme. Numerical studies reveal that the QC method is more accurate and stable.

(3) Compared to the LC method, a wider range of β values (0.5–2.0) can be used in the QC method. Using the same β, the CPU time in computer by the QC method is less than 10 percent more while compared to the CPU time by the LC method. This indicates that if a certain level of accuracy is wanted to be maintained, the QC method is more economical than the LC method, since a larger β value can be selected for the QC method.

Acknowledgment—The authors wish to express their appreciation to the Chung Shan Institute of Science & Technology (CSIST) of Taiwan for the financial support, which makes the research work of the paper possible. In addition, the authors also thank the National Science Council of Taiwan for partly sponsoring the research presented in the paper under contract no. NSC82-0115-E009-435.

REFERENCES

Antes, H. (1985). A boundary element procedure for transient wave propagations in two-dimensional isotropic elastic media. *Finite Elements Anal. Des.* **1,** 313–322.

Banerjee, P. K. (1994). *Boundary Element Methods in Engineering*, McGraw-Hill, London.

Banerjee, P. K., Israil, A. S. M. and Wang, H. C. (1992). Time-domain formulations of BEM for two-dimensional, axisymmetric and three-dimensional transient elastodynamics. In *Advanced Dynamic Analysis by Boundary Element Methods*, chapter 4, pp. 115–153. Elsevier Applied Science, London.

Brebbia, C. A., Telles, J. C. F. and Wrobel, L. C. (1984). *Boundary Element Techniques Theory and Applications in Engineering*, Springer-Verlag, Berlin.

Chen, G. and Zhou, J. (1992). *Boundary Element Methods*, Academic Press, London.

Dominguez, J. and Gallego, R. (1992). Time domain boundary element method for dynamic stress intensity factor computations. *Int. J. Num. Meth. Engng* **33,** 635–647.

Eringen, A. C. and Suhubi, E. S. (1975). *Elastodynamics*, Vol. II, Academic Press, NY.

Graff, K. F. (1975). *Wave Motion in Elastic Solids*, Ohio State University Press, USA.

Israil, A. S. M. and Banerjee, P. K. (1990a). Advanced time-domain formulation of BEM for two-dimensional transient elastodynamics. *Int. J. Num. Meth. Engng* **29,** 1421–1440.

Israil, A. S. M. and Banerjee, P. K. (1990b). Two-dimensional transient wave propagation problems by time-domain BEM. *Int. J. Solids Structures* **26,** 851–864.

Israil, A. S. M. and Banerjee, P. K. (1991). Interior stress calculations in 2-D time-domain transient BEM analysis. *Int. J. Solids Structures* **27,** 915–927.

Manolis, G. D. and Beskos, D. E. (1988). *Boundary Element Methods in Elastodynamics*, Unwin Hyman Ltd, London.

Mansur, W. J. (1983). A time-stepping technique to solve wave propagation problems using the boundary element method. PhD thesis, Southampton University.

Niwa, Y., Fukui, T., Kato, S. and Fujiki, K. (1980). An application of the integral equation method to two-dimensional elastodynamics. In *Theoretical and Applied Mechanics Proceeding of the 28th Japan International Congress of Theoretical and Applied Mechanics*, 1978, pp. 281–290. University of Tokyo Press.

Spyrakos, C. C. and Antes, H. (1986). Time domain boundary element method approaches in elastodynamics: a comparative study. *Computers and Struct.* **24,** 529–535.

Spyrakos, C. C. and Beskos, D. E. (1986). Dynamic response of rigid strip-foundations by a time-domain boundary element method. *Int. J. Num. Meth. Engng* **23,** 1547–1565.

Wang, C. and Takemiya, H. (1992). Analytical elements of time domain BEM for two-dimensional scalar wave problems. *Int. J. Num. Meth. Engng* **33,** 1737–1754.

APPENDIX A

Condensed convoluted kernels of the QC method

These six newly derived forms of the condensed temporal convolution kernels are presented as follows:

A.1. *Equivalent forward-point's condensed constant convoluted displacement kernels of quadratic time step* $[G^{N}_{qCFij}+G^{N-2}_{qCBij}]$ *for* N *is even* $(N = 2K)$

$$[G^{2K}_{qCFij}+G^{2K-2}_{qCBij}]=[G^{2K-1}_{CFij}+G^{2K-2}_{CBij}]=\frac{1}{2\pi\rho}$$

$$\left\{+\left(\frac{\delta_{ij}}{4c_1^2}\right)\left[\cosh^{-1}\left\{\frac{c_1(2K-1)\Delta t}{r}\right\}-\cosh^{-1}\left\{\frac{c_1(2K-3)\Delta t}{r}\right\}\right]\right.$$

$$+\left(\frac{2r_{,i}r_{,j}-\delta_{ij}}{4}\right)\left(\frac{\Delta t}{r}\right)^2\left[(2K-1)\sqrt{(2K-1)^2-\left(\frac{r}{c_1\Delta t}\right)^2}-(2K-3)\sqrt{(2K-3)^2-\left(\frac{r}{c_1\Delta t}\right)^2}\right]$$

$$+\left(\frac{\delta_{ij}}{4c_2^2}\right)\left[\cosh^{-1}\left\{\frac{c_2(2K-1)\Delta t}{r}\right\}-\cosh^{-1}\left\{\frac{c_2(2K-3)\Delta t}{r}\right\}\right]$$

$$\left.-\left(\frac{2r_{,i}r_{,j}-\delta_{ij}}{4}\right)\left(\frac{\Delta t}{r}\right)^2\left[(2K-1)\sqrt{(2K-1)^2-\left(\frac{r}{c_2\Delta t}\right)^2}-(2K-3)\sqrt{(2K-3)^2-\left(\frac{r}{c_2\Delta t}\right)^2}\right]\right\}. \tag{A1}$$

A.2. *First time step of constant convoluted displacement kernels of linear time step* $[G^{N}_{lCFij}+G^{N-1}_{lCBij}]$ *for N is odd* $(N=2K+1)$

$$[G^{2K+1}_{CFij}+G^{2K}_{CBij}]=\frac{1}{2\pi\rho}$$

$$\left\{+\left(\frac{\delta_{ij}}{4c_1^2}\right)\left[\cosh^{-1}\left\{\frac{c_1(2K+1)\Delta t}{r}\right\}-\cosh^{-1}\left\{\frac{c_1(2K-1)\Delta t}{r}\right\}\right]\right.$$

$$+\left(\frac{2r_{,i}r_{,j}-\delta_{ij}}{4}\right)\left(\frac{\Delta t}{r}\right)^2\left[(2K+1)\sqrt{(2K+1)^2-\left(\frac{r}{c_1\Delta t}\right)^2}-(2K-1)\sqrt{(2K-1)^2-\left(\frac{r}{c_1\Delta t}\right)^2}\right]$$

$$+\left(\frac{\delta_{ij}}{4c_2^2}\right)\left[\cosh^{-1}\left\{\frac{c_1(2K+1)\Delta t}{r}\right\}-\cosh^{-1}\left\{\frac{c_2(2K-1)\Delta t}{r}\right\}\right]$$

$$\left.-\left(\frac{2r_{,i}r_{,j}-\delta_{ij}}{4}\right)\left(\frac{\Delta t}{r}\right)^2\left[(2K+1)\sqrt{(2K+1)^2-\left(\frac{r}{c_2\Delta t}\right)^2}-(2K-1)\sqrt{(2K-1)^2-\left(\frac{r}{c_2\Delta t}\right)^2}\right]\right\} \tag{A2}$$

A.3. *Equivalent middle-point's constant convoluted displacement kernels of quadratic time step* $[G^{N}_{qCMij}]=[G^{N}_{lCFij}+G^{N-1}_{lCBij}]$ *for N is even* $(N=2K)$

$$[G^{N}_{qCMij}]=[G^{N}_{CFij}+G^{N-1}_{CBij}]=\frac{1}{2\pi\rho}$$

$$\left\{+\left(\frac{\delta_{ij}}{4c_1^2}\right)\left[\cosh^{-1}\left\{\frac{c_2(N)\Delta t}{r}\right\}-\cosh^{-1}\left\{\frac{c_1(N-2)\Delta t}{r}\right\}\right]\right.$$

$$+\left(\frac{2r_{,i}r_{,j}-\delta_{ij}}{4}\right)\left(\frac{\Delta t}{r}\right)^2\left[(N)\sqrt{(N)^2-\left(\frac{r}{c_1\Delta t}\right)^2}-(N-2)\sqrt{(N-2)^2-\left(\frac{r}{c_1\Delta t}\right)^2}\right]$$

$$+\left(\frac{\delta_{ij}}{4c_2^2}\right)\left[\cosh^{-1}\left\{\frac{c_2(N)\Delta t}{r}\right\}-\cosh^{-1}\left\{\frac{c_2(N-2)\Delta t}{r}\right\}\right]$$

$$\left.+\left(\frac{2r_{,i}r_{,j}-\delta_{ij}}{4}\right)\left(\frac{\Delta t}{r}\right)^2\left[(N)\sqrt{(N)^2-\left(\frac{r}{c_2\Delta t}\right)^2}-(N-2)\sqrt{(N-2)^2-\left(\frac{r}{c_2\Delta t}\right)^2}\right]\right\}. \tag{A3}$$

A.4. *First time step of linear convoluted traction kernels of quadratic time step* $[F^{2K+1}_{LFij}+F^{2K}_{QBij}]$

$$[F^{2K+1}_{LFij}+F^{2K}_{QBij}]=\frac{\mu}{2\pi\rho r}$$

$$\left\{-\left(\frac{A_1}{2c_1^2}\right)\left[2\sqrt{(2K+1)^2-\left(\frac{r}{c_1\Delta t}\right)^2}+(2K-5)\sqrt{(2K)^2-\left(\frac{r}{c_1\Delta t}\right)^2}\right.\right.$$

$$\left.-(2K-1)\sqrt{(2K-2)^2-\left(\frac{r}{c_1\Delta t}\right)^2}\right]$$

$$+\left(\frac{A_2}{3}\right)\left(\frac{\Delta t}{r}\right)^2\left[+2(2K+1)^2\sqrt{(2K+1)^2-\left(\frac{r}{c_1\Delta t}\right)^2}\right.$$

$$\left.+(K-5)(2K)^2\sqrt{(2K)^2-\left(\frac{r}{c_1\Delta t}\right)^2}-(K)(2K-2)^2\sqrt{(2K-2)^2-\left(\frac{r}{c_1\Delta t}\right)^2}\right]$$

$$+\left(\frac{A_2}{6c_1^2}\right)\left[-4\sqrt{(2K+1)^2-\left(\frac{r}{c_1\Delta t}\right)^2}-5(K-2)\sqrt{(2K)^2-\left(\frac{r}{c_1\Delta t}\right)^2}\right.$$

$$\left.+(5K-3)\sqrt{(2K-2)^2-\left(\frac{r}{c_1\Delta t}\right)^2}\right]$$

$$+\left(\frac{2A_1+A_2}{4c_1^2}\right)\left(\frac{r}{c_1\Delta t}\right)^2\left[+\cosh^{-1}\left(\frac{c_1(2K)\Delta t}{r}\right)-\cosh^{-1}\left(\frac{c_1(2K-2)\Delta t}{r}\right)\right]$$

$$+\left(\frac{A_3}{2c_2^2}\right)\left[2\sqrt{(2K+1)^2-\left(\frac{r}{c_2\Delta t}\right)^2}+(2K-5)\sqrt{(2K)^2-\left(\frac{r}{c_2\Delta t}\right)^2}\right.$$

$$\left.-(2K-1)\sqrt{(2K-2)^2-\left(\frac{r}{c_2\Delta t}\right)^2}\right]$$

$$-\left(\frac{A_2}{3}\right)\left(\frac{\Delta t}{r}\right)^2\left[+2(2K+1)^2\sqrt{(2K+1)^2-\left(\frac{r}{c_2\Delta t}\right)^2}\right.$$

$$\left.+(K-5)(2K)^2\sqrt{(2K)^2-\left(\frac{r}{c_2\Delta t}\right)^2}-(K)(2K-2)^2\sqrt{(2K-2)^2-\left(\frac{r}{c_2\Delta t}\right)^2}\right]$$

$$-\left(\frac{A_2}{6c_2^2}\right)\left[-4\sqrt{(2K+1)^2-\left(\frac{r}{c_2\Delta t}\right)^2}-5(K-2)\sqrt{(2K)^2-\left(\frac{r}{c_2\Delta t}\right)^2}\right.$$

$$\left.+(5K-3)\sqrt{(2K-2)^2-\left(\frac{r}{c_2\Delta t}\right)^2}\right]$$

$$-\left(\frac{2A_3+A_2}{4c_2^2}\right)\left(\frac{r}{c_2\Delta t}\right)^2\left[+\cosh^{-1}\left(\frac{c_2(2K)\Delta t}{r}\right)-\cosh^{-1}\left(\frac{c_2(2K-2)\Delta t}{r}\right)\right]\Bigg\}. \tag{A4}$$

A.5. *Forward-point's condensed quadratic convoluted traction kernels of quadratic time step* $[F^{2K}_{QFij}+F^{2K-2}_{QBij}]$

$$[F^{2K}_{QFij}+F^{2K-2}_{QBij}]=\frac{\mu}{2\pi\rho r}$$

$$\left\{+\left(\frac{2A_1+A_2}{4c_1^2}\right)\left(\frac{r}{c_1\Delta t}\right)^2\left[\cosh^{-1}\left(\frac{c_1(2K)\Delta t}{r}\right)-\cosh^{-1}\left(\frac{c_1(2K-4)\Delta t}{r}\right)\right]\right.$$

$$-\left(\frac{A_1}{2c_1^2}\right)\left[(2K-1)\sqrt{(2K)^2-\left(\frac{r}{c_1\Delta t}\right)^2}-6\sqrt{(2K-2)^2-\left(\frac{r}{c_1\Delta t}\right)^2}\right.$$

$$\left.-(2K-3)\sqrt{(2K-4)^2-\left(\frac{r}{c_1\Delta t}\right)^2}\right]$$

$$+\left(\frac{A_2}{6c_1^2}\right)\left[-(5K-2)\sqrt{(2K)^2-\left(\frac{r}{c_1\Delta t}\right)^2}+12\sqrt{(2K-2)^2-\left(\frac{r}{c_1\Delta t}\right)^2}\right.$$

$$\left.+(5K-8)\sqrt{(2K-4)^2-\left(\frac{r}{c_1\Delta t}\right)^2}\right]$$

$$+\left(\frac{A_2}{3}\right)\left(\frac{\Delta t}{r}\right)^2\left[(K-1)(2K)^2\sqrt{(2K)^2-\left(\frac{r}{c_1\Delta t}\right)^2}-6(2K-2)^2\sqrt{(2K-2)^2-\left(\frac{r}{c_1\Delta t}\right)^2}\right.$$

$$\left.-(K-1)(2K-4)^2\sqrt{(2K-4)^2-\left(\frac{r}{c_1\Delta t}\right)^2}\right]$$

$$-\left(\frac{2A_3+A_2}{4c_2^2}\right)\left(\frac{r}{c_2\Delta t}\right)^2\left[\cosh^{-1}\left(\frac{c_2(2K)\Delta t}{r}\right)-\cosh^{-1}\left(\frac{c_2(2K-4)\Delta t}{r}\right)\right]$$

$$+\left(\frac{A_3}{2c_2^2}\right)\left[(2K-1)\sqrt{(2K)^2-\left(\frac{r}{c_2\Delta t}\right)^2}-6\sqrt{(2K-2)^2-\left(\frac{r}{c_2\Delta t}\right)^2}\right.$$

$$-(2K-3)\sqrt{(2K-4)^2-\left(\frac{r}{c_2\Delta t}\right)^2}\Bigg]$$

$$-\left(\frac{A_2}{6c_2^2}\right)\Bigg[-(5K-2)\sqrt{(2K)^2-\left(\frac{r}{c_2\Delta t}\right)^2}+12\sqrt{(2K-2)^2-\left(\frac{r}{c_2\Delta t}\right)^2}$$

$$+(5K-8)\sqrt{(2K-4)^2-\left(\frac{r}{c_2\Delta t}\right)^2}\Bigg]$$

$$-\left(\frac{A_2}{3}\right)\left(\frac{\Delta t}{r}\right)^2\Bigg[(K-1)(2K)^2\sqrt{(2K)^2-\left(\frac{r}{c_2\Delta t}\right)^2}-6(2K-2)^2\sqrt{(2K-2)^2-\left(\frac{r}{c_2\Delta t}\right)^2}$$

$$-(K-1)(2K-4)^2\sqrt{(2K-4)^2-\left(\frac{r}{c_2\Delta t}\right)^2}\Bigg]\Bigg\}. \tag{A5}$$

A.6. *Middle point's quadratic convoluted traction kernels of quadratic time step* $[F^{2K}_{QMij}]$

$$[F^{2K}_{QMij}]=\frac{\mu}{2\pi\rho r}$$

$$\Bigg\{-\left(\frac{A_1}{c_1^2}\right)\Bigg[-(2K-2)\sqrt{(2K)^2-\left(\frac{r}{c_1\Delta t}\right)^2}+(2K)\sqrt{(2K-2)^2-\left(\frac{r}{c_1\Delta t}\right)^2}\Bigg]$$

$$+\left(\frac{2A_2}{3}\right)\left(\frac{\Delta t}{r}\right)^2\Bigg[-(K-2)(2K)^2\sqrt{(2K)^2-\left(\frac{r}{c_1\Delta t}\right)^2}+(K+1)(2K-2)^2\sqrt{(2K-2)^2-\left(\frac{r}{c_1\Delta t}\right)^2}\Bigg]$$

$$+\left(\frac{A_2}{3c_1^2}\right)\Bigg[+(5K-4)\sqrt{(2K)^2-\left(\frac{r}{c_1\Delta t}\right)^2}-(5K-1)\sqrt{(2K-2)^2-\left(\frac{r}{c_1\Delta t}\right)^2}\Bigg]$$

$$+\left(\frac{2A_1+A_2}{2c_1^2}\right)\left(\frac{r}{c_1\Delta t}\right)^2\Bigg[-\cosh^{-1}\left(\frac{c_1(2K)\Delta t}{r}\right)+\cosh^{-1}\left(\frac{c_1(2K-2)\Delta t}{r}\right)\Bigg]$$

$$+\left(\frac{A_3}{c_2^2}\right)\Bigg[-(2K-2)\sqrt{(2K)^2-\left(\frac{r}{c_2\Delta t}\right)^2}+(2K)\sqrt{(2K-2)^2-\left(\frac{r}{c_2\Delta t}\right)^2}\Bigg]$$

$$-\left(\frac{2A_2}{3}\right)\left(\frac{\Delta t}{r}\right)^2\Bigg[-(K-2)(2K)^2\sqrt{(2K)^2-\left(\frac{r}{c_2\Delta t}\right)^2}+(K+1)(2K-2)^2\sqrt{(2K-2)^2-\left(\frac{r}{c_2\Delta t}\right)^2}\Bigg]$$

$$-\left(\frac{A_2}{3c_2^2}\right)\Bigg[+(5K-4)\sqrt{(2K)^2-\left(\frac{r}{c_2\Delta t}\right)^2}-(5K-1)\sqrt{(2K-2)^2-\left(\frac{r}{c_2\Delta t}\right)^2}\Bigg]$$

$$-\left(\frac{2A_3+A_2}{2c_2^2}\right)\left(\frac{r}{c_2\Delta t}\right)^2\Bigg[-\cosh^{-1}\left(\frac{c_2(2K)\Delta t}{r}\right)+\cosh^{-1}\left(\frac{c_2(2K-2)\Delta t}{r}\right)\Bigg]\Bigg\}. \tag{A6}$$

APPENDIX B

Reimann convolution integral

$$G_{ij}(\xi,\tau;\mathbf{x},t)*t_j(\mathbf{x},t)=\int_0^t G_{ij}(\xi,\tau;\mathbf{x},t)t_j(\mathbf{x},\tau)\,d\tau=\int_0^t G_{ij}(\xi,0;\mathbf{x},t-\tau)t_j(\mathbf{x},\tau)\,d\tau \tag{B1}$$

$$F_{ij}(\xi,\tau;\mathbf{x},t)*u_j(\mathbf{x},t)=\int_0^t F_{ij}(\xi,\tau;\mathbf{x},t)u_j(\mathbf{x},\tau)\,d\tau=\int_0^t F_{ij}(\xi,0;\mathbf{x},t-\tau)u_j(\mathbf{x},\tau)\,d\tau. \tag{B2}$$